Morphological Transitions of Wetting Layers on Structured Surfaces

Peter Lenz and Reinhard Lipowsky
Max-Planck-Institut für Kolloid- und Grenzflächenforschung, Kantstrasse 55, D-14513 Teltow-Seehof, Germany
(Received 8 September 1997)

The morphology of wetting layers on structured or imprinted surfaces is determined by the geometry of the underlying surface domains. Droplets which cover a single domain exhibit contact angles which do not satisfy Young's equation. For surface patterns consisting of many surface domains, the wetting layer exhibits several distinct morphologies (homogeneous droplet patterns, heterogeneous droplet patterns, film states) and may undergo morphological transitions between these different states. The latter transitions exhibit spontaneous symmetry breaking. [S0031-9007(98)05366-6]

PACS numbers: 68.45.Gd, 68.10.Cr

Several experimental methods are available by which one can create structured or imprinted surfaces with domain sizes of a few micrometers. Three examples are (i) elastomer stamps by which one can create patterns of hydrophobic alkanethiol on metal surfaces [1], (ii) vapor deposition through grids which cover part of the surface [2], and (iii) photolithography of amphiphilic monolayers which contain photosensitive molecular groups [3].

If such a structured surface is in contact with a liquid, the corresponding interface has a position-dependent free energy which reflects the underlying surface pattern. In order to be specific, let us consider a surface which consists of hydrophilic domains in a hydrophobic matrix and let us place a thin wetting layer of water [4] onto this surface. The water wants to wet the hydrophilic domains but wants to dewet the hydrophobic matrix, respectively. As a result, the surface pattern will modulate the shape of the water layer and thus will affect its morphology.

In this Letter, we will theoretically study this interplay between the pattern of surface domains and the wetting layer morphology. We will first show that, for a *single* surface domain, one must distinguish three different droplet regimes, denoted by 1, 2, and 3, depending on the hydrophilicity and hydrophobicity of the two types of surface domains. If these domains are strongly hydrophilic and strongly hydrophobic, respectively, all droplets belong to the intermediate regime 2. The latter regime is unusual since the corresponding droplets are characterized by contact angles which do *not* satisfy the well-known Young equation.

For a surface pattern consisting of *many* surface domains, we find that the wetting layer can exhibit several distinct morphologies: (i) a homogeneous droplet pattern where all droplets have the same size; (ii) a heterogeneous droplet pattern characterized by one large and many small droplets; and (iii) a film state for which the wetting layer covers both the hydrophilic and the hydrophobic surface regions. The relevant parameters which determine the corresponding phase diagram are (a) the water volume v per hydrophilic domain and (b) the area fraction X of the hydrophilic domains; see Fig. 1. As one moves across the phase boundaries, the wetting layer undergoes transitions between these different morphologies.

These morphologies represent equilibrium states of a certain amount of liquid and are obtained by minimization of the interfacial free energy subject to the constraint of constant liquid volume. This statistical ensemble describes three somewhat different physical situations: (i) Liquid-vapor systems at two-phase coexistence for which the amount of liquid is controlled by the total volume of the system and the total number of particles. (ii) Liquid-vapor systems off coexistence for which the vapor phase in the bulk is slightly supersaturated but still (meta)stable as studied experimentally, e.g., in Refs. [2,3]. At the hydrophilic surface domains, the nucleation barriers are strongly reduced, however, and the liquid starts to condense at those domains. In this case, the amount of liquid increases with time, but if this growth process is slow, the resulting time evolution of the droplet morphology will resemble a sequence of equilibrium states as considered here. (iii) Nonvolatile liquids which are placed onto the structured surface by pipettes or other means; see, e.g., Ref. [1]. For this latter case, we determine the most probable droplet morphology. In practice, the droplets in case (iii) will be typically in a metastable state which depends on the preparation

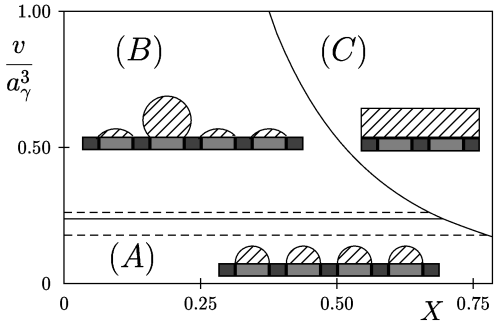

FIG. 1. Droplet morphologies for circular hydrophilic domains with diameter a_γ as determined by the reduced volume v/a_γ^3 of the liquid and the area fraction X of the hydrophilic domains. The numerical values are for four domains.

 0031-9007/98/80(9)/1920(4)$15.00

method, and one has to perturb the system externally in order to attain a different morphology of lower free energy [5].

In this Letter, we give a brief summary of our results. The derivation of these results is somewhat lengthy and will be given in a forthcoming paper [6]. We focus on droplets in the micrometer range for which one may ignore (i) the effects of gravity which are important for millimeter-sized drops [7–9] and (ii) the details of intermolecular interactions such as, e.g., van der Waals forces which lead to thickness-dependent interfacial tensions for thin wetting layers with thickness in the nanometer range [10]. van der Waals forces have been explicitly considered for wetting layers on surfaces which consist of two semi-infinite surface regions [11] and for wetting layers which bridge the gap between two parallel surfaces with striped surface domains [12].

To proceed, we will denote the vapor and the liquid phase by (α) and (β), and the hydrophilic and hydrophobic surface regions by (γ) and (δ), respectively. The interfacial region between phase (i) and phase (j) has surface area A_{ij} and interfacial tension Σ_{ij}. The equilibrium state corresponds to the global minimum of the total interfacial free energy as given by

$$F = \Sigma_{\alpha\beta}A_{\alpha\beta} + \Sigma_{\alpha\gamma}A_{\alpha\gamma} + \Sigma_{\alpha\delta}A_{\alpha\delta} + \Sigma_{\beta\gamma}A_{\beta\gamma} + \Sigma_{\beta\delta}A_{\beta\delta}\,. \quad (1)$$

The two surface regions are characterized by two contact angles θ_γ and θ_δ which satisfy the usual Young relations

$$\frac{\Sigma_{\alpha\gamma} - \Sigma_{\beta\gamma}}{\Sigma_{\alpha\beta}} = \cos\theta_\gamma \quad \text{and} \quad \frac{\Sigma_{\alpha\delta} - \Sigma_{\beta\delta}}{\Sigma_{\alpha\beta}} = \cos\theta_\delta\,. \quad (2)$$

Here, we have implicitly ignored corrections arising from the line tension of the contact or triple phase line which will be relevant for droplets on smaller scales; for a recent discussion, see [13]. Note that a completely hydrophilic (γ) domain corresponds to $\theta_\gamma = 0$ and a completely hydrophobic (δ) domain to $\theta_\delta = \pi$. In general, we will assume $0 \le \theta_\gamma < \pi/2 < \theta_\delta \le \pi$.

The two contact angles θ_γ and θ_δ apply to contact lines which are located *within* the surface domains, i.e., away from the $(\gamma\delta)$ domain boundaries. These domain boundaries have a certain width or fuzziness which depends on the experimental procedure by which the surface has been structured or imprinted.

Within the transition region from a (γ) to a (δ) domain, the interfacial free energies between the two fluid phases and the surface will gradually change, and we are led to consider *position-dependent* interfacial free energies $[\Sigma_{\alpha s}(\mathbf{x}), \Sigma_{\beta s}(\mathbf{x})]$ which vary with the surface coordinate $\mathbf{x}$ and which interpolate between the limiting values $(\Sigma_{\alpha\gamma}, \Sigma_{\beta\gamma})$ and $(\Sigma_{\alpha\delta}, \Sigma_{\beta\delta})$ within the (γ) and the (δ) domain, respectively.

Explicit minimization of the total free energy of a droplet shows that such a gradual change leads to a local, position-dependent contact angle $\theta(\mathbf{x})$ which satisfies the generalized Young equation

$$[\Sigma_{\alpha s}(\mathbf{x}) - \Sigma_{\beta s}(\mathbf{x})]/\Sigma_{\alpha\beta} = \cos\theta(\mathbf{x})\,. \quad (3)$$

Thus, as the contact line moves through this transition region, the contact angle will change gradually from $\theta = \theta_\gamma$ to $\theta = \theta_\delta$. As mentioned, we will consider the limit in which the width of this transition region becomes small; in this limit, the position-dependent contact angle becomes a step function with a jump at the domain boundary. Thus, as soon as the contact line has reached the domain boundary, the contact angle θ of the droplet is no longer fixed but can have any value within the interval $\theta_\gamma < \theta < \theta_\delta$.

Circular domains.—First consider a droplet on one circular hydrophilic domain (γ) within a hydrophobic surface (δ). The diameter of the domain will be denoted by a_γ. Such a droplet forms a spherical cap with radius R, contact angle θ, and volume

$$V_d(R,\theta) = \pi R^3(1 - \cos\theta)^2(2 + \cos\theta)/3\,. \quad (4)$$

The surface areas of the $(\alpha\beta)$ and the (βs) interfaces with $s = \gamma$ or δ are given by $A_{\alpha\beta} = 2\pi R^2(1 - \cos\theta)$ and $A_{\beta s} = \pi R^2 \sin^2\theta$, respectively. The latter area $A_{\beta s}$ will be referred to as the contact area of the droplet.

Depending on the droplet volume V three different regimes can be distinguished; compare Fig. 2.

(i) Regime 1: For $V < V_d(a_\gamma/2\sin\theta_\gamma, \theta_\gamma)$, the droplet wets only part of the (γ) domain. The contact angle is fixed to the value $\theta = \theta_\gamma$ and thus obeys the Young equation. The contact area increases with increasing V.

(ii) Regime 2: For $V_d(a_\gamma/2\sin\theta_\gamma, \theta_\gamma) \le V \le V_d(a_\gamma/2\sin\theta_\delta, \theta_\delta)$, the droplet covers the (γ) domain completely; i.e., the contact area is fixed. The Young equation is not satisfied, and the contact angle θ with $\theta_\gamma \le \theta \le \theta_\delta$ increases with V.

(iii) Regime 3: For $V_d(a_\gamma/2\sin\theta_\delta, \theta_\delta) < V$, the contact area exceeds the area of the (γ) domain and increases with V. The contact angle is now fixed at the value $\theta = \theta_\delta$.

In order to simplify the following discussion we will focus on the limiting case $\theta_\gamma = 0$ and $\theta_\delta = \pi$. We are then left with regime 2 for all droplet volumes.

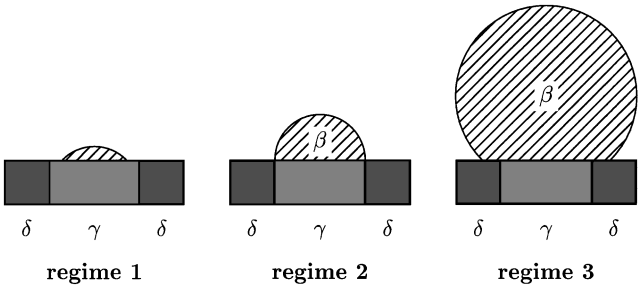

FIG. 2. Depending on the droplet volume, the droplet state belongs to regime 1, 2, or 3. The contact angle is equal to θ_γ and θ_δ in regimes 1 and 3, respectively.

Two-dimensional lattice of hydrophilic domains.—Next a lattice of N circular (γ) domains will be considered. These domains are placed periodically on the hydrophobic surface (δ). To be specific, we will focus on the case where these circular domains form a square lattice with lattice constant a.

If the total liquid volume V is small, the equilibrium state consists of N identical droplets covering the N (γ) domains. Thus, one has a homogeneous droplet pattern denoted by (A) in Fig. 1 for which all droplets have identical contact angle θ and identical droplet volume $v = V/N$. As the volume is increased, the droplets grow until the contact angle reaches a critical value $\theta = \theta^*_{AB}$ at which the system undergoes a transition to another equilibrium state denoted by (B) in Fig. 1. The latter state is not translationally invariant and consists of one large and $(N - 1)$ small droplets.

Thus, at this critical contact angle $\theta = \theta^*_{AB}(N)$, rearrangement of the liquid lowers the interfacial free energy. Formally, this can be proven by assigning a volume fraction x_n to each droplet n. By varying the free energy under the constraint $\sum_{n=1}^{N} x_n = 1$, one finds that for $\theta > \theta^*_{AB}(N)$ the global minimum of the free energy is then given by a heterogeneous droplet pattern. It consists of one large droplet with contact angle $\theta_{\rm la} > \pi/2$ and $(N - 1)$ small droplets with contact angle $\theta_{\rm sm} = \pi - \theta_{\rm la} < \pi/2$; see Fig. 1. Since the large droplet can be located on any of the N domains, the symmetry of the (A) state is spontaneously broken and the (B) state is N-fold degenerate. In addition, there is a whole spectrum of stationary states consisting of $N_{\rm sm}$ small and $N_{\rm la}$ large droplets with $N_{\rm sm} + N_{\rm la} = N$ [6].

The transition from the homogeneous to the heterogeneous pattern is continuous for $N = 2$ but discontinuous for $N > 2$. For $N = 2$, the critical contact angle $\theta^*_{AB}(N = 2) = \pi/2$. For $N > 2$, one has a hysteresis loop for the contact angle range $\theta^{\rm min}_{AB}(N) < \theta < \theta^{\rm max}_{AB}(N)$ where $\theta^{\rm max}_{AB}(N)$ has the universal value

$$\theta^{\rm max}_{AB}(N) = \pi/2 \qquad \text{for all } N\,. \tag{5}$$

In the range $\theta^{\rm min}_{AB} < \theta < \theta^*_{AB}$, the homogeneous and the heterogeneous droplet patterns are stable and metastable, respectively. For $\theta^*_{AB} < \theta < \theta^{\rm max}_{AB}$, on the other hand, these two states have exchanged their stability. For large N, one finds after some computation that the contact angles $\theta^{\rm min}_{AB}$ and θ^*_{AB} have the asymptotic behavior

$$\theta^{\rm min}_{AB}(N) \approx 8/3N^{1/4}, \quad \theta^*_{AB}(N) \approx 4/(3N)^{1/4}. \tag{6}$$

Under suitable experimental conditions, the wetting layer can exhibit a third morphology. It is given by a flat film corresponding to a completely wetted state. This state can be experimentally realized by appropriate boundary conditions. For instance, one may add confining walls of phase (ε) perpendicular to the structured surface with contact angle $\theta_\varepsilon \simeq \pi/2$. Under such experimental circumstances, it will be energetically favorable for the liquid to build a flat film as soon as its volume V exceeds a critical value V^*. At $V = V^*$, the wetting layer undergoes a discontinuous transition from one of the droplet states to the film state denoted by (C) in Fig. 1.

At the transition point, the partially wet state is given either by the homogeneous droplet pattern (A) or by the heterogeneous droplet pattern (B). The geometry of the domain lattice, characterized by the area fraction $X \equiv \pi a_\gamma^2/4a^2$, of the hydrophilic domains determines which pattern undergoes the transition. For a hydrophobic surface with sufficiently low $X < X^*_{ABC}$, the film state is energetically very unfavorable. Hence, as the volume is increased for $X < X^*_{ABC}$, the droplets will attain the contact angle $\theta = \theta^*_{AB}$ and will then be transformed into the state (B). As the volume is further increased, the larger droplet grows, whereas the smaller ones shrink. But finally, the area of the $(\alpha\beta)$ interfaces of this droplet state will become so large that the heterogeneous droplet pattern (B) undergoes a transition towards the film state (C) at the critical volume $V = V^*_{BC}$. In contrast, for a hydrophilic surface with $X > X^*_{ABC}$, the transition takes place directly between the homogeneous droplet state (A) and the flat film (C) at the critical volume V^*_{AC} [14].

For large N, the value of X^*_{ABC} behaves as

$$X^*_{ABC}(N) \approx 1 - 2/(3N)^{1/2}. \tag{7}$$

For the circular domains considered here, the area fraction $X = \pi a_\gamma^2/4a^2$ is, however, restricted to $X \le \pi/4 \simeq 0.79$ which implies that the (AC) transition is not accessible for large N.

If the contact angles of the (γ) and (δ) domains satisfy $\theta_\gamma > 0$ and $\theta_\delta < \pi$, the transition at $V = V^*_{AC}$ or V^*_{BC} can take place in regime 1, 2, or 3, depending on the area fraction X [6].

Striped domains.—Next, consider a hydrophilic stripe (γ) on a hydrophobic surface (δ). The (γ) stripe has the width a_γ and the longitudinal extension L with $L \gg a_\gamma$.

Because of the cylindrical symmetry, the droplet on such a stripe forms a channel and its surface has the shape of a cylindrical segment with radius R and contact angle θ. Its surface areas are given by $A_{\alpha\beta} = 2\theta RL$ and $A_{\beta s} = 2RL \sin\theta$ with $s = \gamma$ or δ. The volume is given by $V_d(R, \theta) = (\theta - \frac{1}{2}\sin 2\theta)R^2L$.

There are again three different droplet regimes 1, 2, and 3 in close analogy to the case of circular domains. As in the latter case, we will focus on regime 2 for which the contact area is equal to the area of the hydrophilic stripe and the contact angle θ can vary from 0 to π.

Periodic grid of striped domains.—Here the surface consists of N parallel stripes of (γ) phase which have the width a_γ. The separation of the stripes is denoted by a_δ, and the whole array has the period $a = a_\gamma + a_\delta$.

For the droplet regime 2 with $\theta_\gamma = 0$ and $\theta_\delta = \pi$, one finds again three different morphologies (A), (B), and (C) as for circular domains. The morphology (A) consists of identical channels each of which covers a single hydrophilic (γ) domain, (B) consists of one large channel and $(N - 1)$ small ones, and (C) corresponds to film states which cover the whole surface.

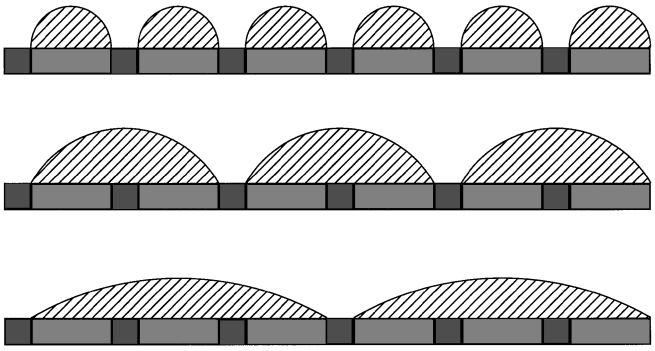

FIG. 3. For striped domains, the transition from the channel state (A) (top) to the film state may proceed via the intermediate states (A_2) (middle) and (A_3) (bottom) consisting of channels which cover 2 and 3 hydrophilic (γ) domains, respectively.

The transition from the (A) to the (B) state has the same features as for circular domains. The transition takes place at the critical contact angle $\theta = \theta^*_{AB}(N)$. The homogeneous channel state remains metastable up to $\theta = \theta^{\max}_{AB}$ which has again the universal value $\theta^{\max}_{AB} = \pi/2$ for all N as in (5). The heterogeneous channel state stays metastable down to $\theta = \theta^{\min}_{AB}(N)$. For large N, one finds the asymptotic behavior

$$\theta^{\min}_{AB}(N) \approx \left(\frac{81\pi}{8N}\right)^{1/3}, \qquad \theta^*_{AB}(N) \approx \left(\frac{81\pi}{4N}\right)^{1/3}. \quad (8)$$

For striped domains, the area fraction of the hydrophilic domains is given by $X = a_\gamma/a$ which now satisfies $X \leq 1$. Thus, the transition from the (A) to the (C) state is now accessible even for large N. However, the corresponding transition region may now contain new states (A_m) consisting of identical m channels, each of which covers m hydrophilic (γ) domains; see Fig. 3. As the volume and, thus, the contact angle are increased, one first has a transition from (A) to (A_2), then from (A_2) to (A_3) and so on. The states have lower free energy because the reduction of the $(\alpha\beta)$ interfacial area overcompensates the energetic cost of wetting a (δ) stripe. Thus, one has a sequence of critical volumes V^*_m or critical contact angles θ^*_m with $m = 1, 2, \ldots$, at which the channel pattern undergoes morphological transitions from state (A_m) to state (A_{m+1}) [where (A_1) corresponds to (A)].

In addition, there is another new feature for striped domains: The channels can undergo a longitudinal instability and develop a bulge for sufficiently large volume which has been observed experimentally [2]. Theoretical work on this longitudinal instability is in progress and will be described elsewhere.

In summary, we have shown that wetting layers on structured surfaces undergo transitions between different morphologies. Both for droplets on circular surface domains and for channels on striped domains, homogeneous patterns (A) of identical droplets or channels, heterogeneous patterns (B), and film states (C) have been identified. The transitions between these states are characterized by spontaneous symmetry breaking. All of these states should be experimentally accessible.

The theoretical approach described here can be applied to a number of related problems. One example is provided by hydrophobic domains on a hydrophilic surface. In the latter case, one obtains perforated or partially dewetted layers which again undergo morphological transitions as one varies a control parameter. Similar transitions also occur for liquid layers which are placed between *two* structured surfaces. Finally, in all of these cases, one may also study nanometer domains and droplets, if one includes contact line tensions and thickness-dependent interfacial tensions.

We thank S. Herminghaus and H. Gau for stimulating discussions.

[1] J. Drelich, J. D. Miller, A. Kumar, and G. M. Whitesides, Colloids Surf. A **93**, 1 (1994).
[2] S. Herminghaus, K. Jacobs, S. Schlagowski, H. Gau, and W. Mönch (to be published).
[3] G. Möller, M. Harke, and H. Motschmann (to be published).
[4] In general, our theory can be applied to any two-phase system in contact with a structured surface.
[5] In the case of a large nonvolatile droplet which covers many surface domains, the metastable states can be distinguished by different configurations of the contact or triple phase line which traverses both hydrophilic and hydrophobic surface regions; see, e.g., E. L. Decker and S. Garoff, Langmuir **12**, 2100 (1996); A. Paterson, M. Fermigier, P. Jenffer, and L. Limat, Phys. Rev. E **51**, 1291 (1995).
[6] P. Lenz and R. Lipowsky (to be published).
[7] G. I. Taylor and D. H. Michael, J. Fluid Mech. **58**, 625 (1973).
[8] A. Sharma and E. Ruckenstein, J. Colloid Interface Sci. **133**, 358 (1989).
[9] F. Brochard-Wyart and J. Daillant, Can. J. Phys. **68**, 1084 (1990).
[10] See, e.g., R. Lipowsky, Phys. Rev. Lett. **52**, 1429 (1984); R. Lipowsky and M. E. Fisher, Phys. Rev. B **36**, 2126 (1987).
[11] W. Koch, S. Dietrich, and M. Napiorkowski, Phys. Rev. E **51**, 3300 (1995).
[12] M. Schön and D. J. Diestler, Chem. Phys. Lett. **270**, 339 (1997).
[13] B. Widom, J. Phys. Chem. **99**, 2803 (1995).
[14] Finite $N < \infty$ has been implicitly assumed. For large V the ground state is then given by a (macroscopic) film. The case $N = \infty$ can be achieved by taking the thermodynamic limit of large V and large N with $V/N = \text{const}$. In the latter case, one will end up in the heterogeneous droplet regime with $\theta_{\text{la}} = \pi$ and $\theta_{\text{sm}} = 0$.